

Nuclear Fusion in Collapsing Bubbles—Is It There? An Attempt to Repeat the Observation of Nuclear Emissions from Sonoluminescence

D. Shapira and M. Saltmarsh

Physics Division, Oak Ridge National Laboratory, Oak Ridge, Tennessee

(Received 17 July 2002; published 19 August 2002)

We have repeated the experiment of Taleyarkhan *et al.* [Science **295**, 1868 (2002)] in an attempt to detect the emission of neutrons from *d-d* fusion during bubble collapse in deuterated acetone. Using the same cavitation apparatus, a more sophisticated data acquisition system, and a larger scintillator detector, we find no evidence for 2.5-MeV neutron emission correlated with sonoluminescence from collapsing bubbles. Any neutron emission that might occur is at least 4 orders of magnitude too small to explain the tritium production reported in Taleyarkhan *et al.* as being due to *d-d* fusion. We show that proper allowance for random coincidence rates in such experiments requires the simultaneous measurement of the count rates in the individual detectors.

DOI: 10.1103/PhysRevLett.89.104302

PACS numbers: 78.60.Mq, 25.45.-z, 28.20.-v, 28.52.-s

Sonoluminescence (SL) occurs when light is emitted from collapsing bubbles in a liquid subjected to an acoustic field. Under the right conditions, the bubbles can collapse rapidly, producing internal temperatures and pressures high enough that short (few ps) light flashes are emitted [1–3]. The spectrum of the emitted light indicates that the surface of the emitting bubble may be hotter than the surface of the sun [4]. It has been proposed [5] that the interior of the bubble may be hot and dense enough to facilitate thermonuclear fusion. In a recent paper Taleyarkhan *et al.* [6] reported the possible observation of *d-d* fusion events occurring in collapsing bubbles formed by cavitation in deuterated acetone. Cavitation bubbles were seeded by pulses of neutrons from a 14-MeV pulsed-neutron generator (PNG) phased to the acoustic wave, but with frequency divided by 100. We repeated the original experiment in collaboration with some of the authors of Ref. [6] using the same equipment, with the exception of the scintillation detectors, for which we substituted a larger one (3 l) based on NE213 liquid scintillator, and a more sophisticated data acquisition system.

Our experiment focused on the detection of nuclear emissions from the sonoluminescent bubbles. No attempt was made to measure tritium production. We note that the reported level of tritium production, if it were due to *d-d* fusion, would have been accompanied by an easily detectable level (10^6 s^{-1}) of 2.5 MeV neutron emission. This is the same strength as the 14-MeV neutron generator used.

The physical setup, shown in Fig. 1, was identical to the original experiment. We added a large *n γ* detector based on NE213 liquid scintillator. The flask of deuterated acetone, ~ 6.5 cm in diam, was enclosed within a Plexiglas box with 6 mm walls. In addition, there was a pack of refrigeration materials 3 cm thick between the flask and the Plexiglas wall. We used conventional particle-counting systems and event-by-event data recording with a computer based data acquisition system [7]. The operating condition of the cavitation apparatus was set by the authors of Ref. [6] to be identical to that used in their experiment.

The discriminator threshold for the sonoluminescence light detector was set up as specified in Ref. [6]. Our neutron detector threshold, set by a fast discriminator, was calibrated by comparison with the pulse-height spectrum from a Pu-Be source available during the experiment. The relative response to a Pu-Be source and a ^{60}Co source was checked prior to the experiment. The ^{60}Co Compton edge (equivalent to a 1-MeV electron) was found to be at a fraction 0.29 of the Pu-Be edge. The threshold used in the experiment was at an equivalent electron energy of 270 keV. Using published [8] curves of light output, we estimate our threshold to have been at an equivalent neutron energy of 1.2 MeV, well below the threshold for 2.5-MeV neutron detection. Approximating the geometry of our detector as a slab of area 285 cm^2 and average thickness 10 cm, we obtain a rough estimate of its intrinsic

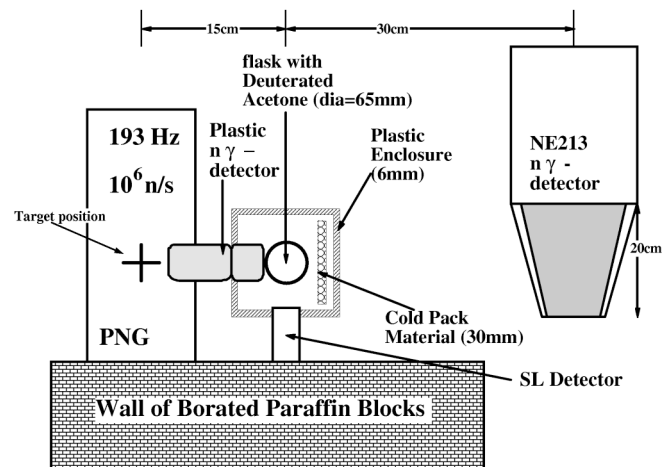


FIG. 1. The experimental setup was placed on top of a steel table standing about 80 cm above the concrete floor. The borated paraffin shield was about 100 cm high and 20 cm deep. The PNG, the SL light detector, and the large scintillator were placed in a single horizontal plane. The plastic scintillator was placed at an angle out of plane.

efficiency. The mean free path of a 2.5 MeV neutron in NE213 is 5 cm so the probability of an n - p scattering (0.57) is given by the total cross-section ratios for H and C corrected for their relative abundance in NE213 [9]. Correcting this probability to allow for our finite threshold (a factor of 0.52) gives an estimated efficiency of 0.3. We estimate the uncertainty in this figure to be about a factor of 2.

The data acquisition system recorded three types of events: $n\gamma$ singles: any pulse from the $n\gamma$ detector above the fast (lowest) threshold; SL singles: any pulse from the SL detector above the threshold; SL- $n\gamma$ coincidences: defined by a $\pm 10 \mu\text{s}$ window triggered by the SL signal.

For each event listed above, the following information was digitized and recorded: the time relative to the last PNG trigger pulse using a 1-MHz clock ($1 \mu\text{s}$ time resolution); the pulse heights from the SL and $n\gamma$ detectors; an $n\gamma$ discrimination signal; for each coincidence event the time difference between the $n\gamma$ and SL signals was recorded with time resolution near 10 ns.

The nominal output of the PNG was 10^6 n/s ($\sim 5000 \text{ n/pulse}$). The pulse width from the PNG was measured to be about $12 \mu\text{s}$. Thus, the event rate seen by the electronics during the PNG pulse was high and would

have resulted in unacceptable counting losses in the period immediately after the start of the neutron pulse. To avoid this, a blocking signal was used to veto all counts from the $n\gamma$ detector for $20 \mu\text{s}$ after the onset of the PNG trigger pulse. In addition, the event rate from $n\gamma$ singles was reduced by looking only at every eighth pulse, thereby reducing the dead time for the data acquisition systems to $\leq 3\%$. The division by eight was not applied to the pulses used to identify the coincidences.

Figure 2 shows the distribution of events recorded during the experiment, as a function of the time from the preceding PNG pulse. No $n\gamma$ discrimination is activated for these plots.

The background seen by the $n\gamma$ detector has three components, which have different time structure (Fig. 2) and pulse-height spectra (Fig. 3). In region A during the $12 \mu\text{s}$ PNG pulse, there is the isolated peak due to 14 MeV neutrons, which we normally block out. In the absence of blocking the instantaneous rate would have been $\sim 10^6 \text{ s}^{-1}$. The pulse-height spectrum from this component, taken with reduced PNG intensity, is shown in Fig. 3(a). Regions B and C, immediately after the PNG pulse, show an exponentially decaying tail (Fig. 2). These events we identify as essentially all gammas, resulting

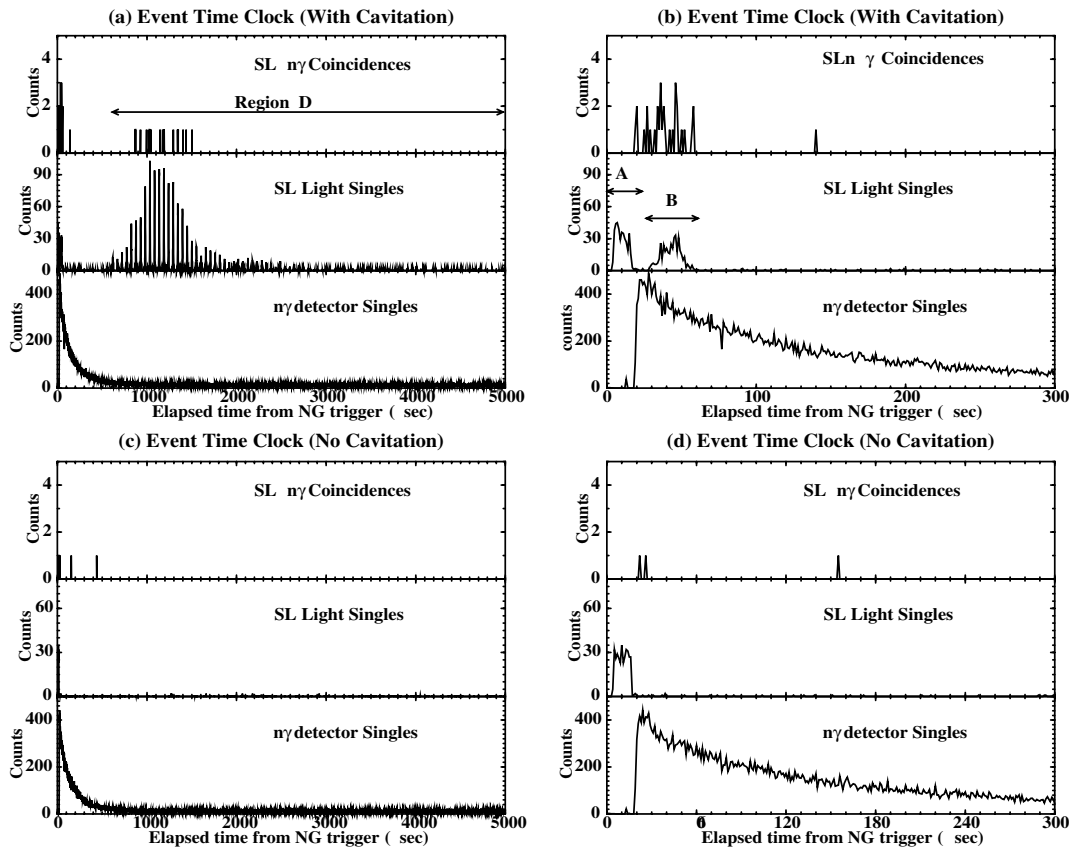


FIG. 2. Event occurrence time relative to PNG trigger time recorded for $n\gamma$ singles, SL light emission singles, and the SL- n/γ coincidences. The data shown on the right are with an expanded time scale. Parts (a) and (b) show data taken with cavitation and (c) and (d) data taken without cavitation. The figure represents counts accumulated in $\sim 1 \text{ h}$ runs. We look at the data rates in four distinct regions marked in the figure as A, B, and D and $62 \mu\text{s} \leq C \leq 539 \mu\text{s}$ (not marked)

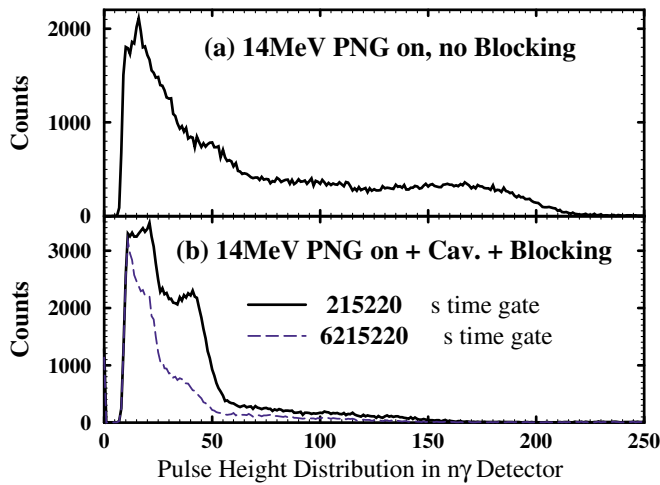


FIG. 3 (color online). Pulse-height spectra recorded with the same n/γ detector settings. (a) shows a 14 MeV neutron spectrum taken with reduced output from the PNG and no blocking signal. The 14-MeV edge is around channel 200, the threshold around channel 8/9. The pulse-height spectra taken during data runs with blocking turned on are shown in (b). The spectrum from all events (solid line) show a distinctive edge around channel 50, consistent with 2.2 MeV n - p capture γ s.

from slow scattered (room return) neutrons being captured on various nuclei in the scintillator and surrounding material. The instantaneous count rate in this region is as high as 4000 s^{-1} immediately after the PNG pulse, dropping off with a time constant $\sim 140 \mu\text{s}$. This component we expect to scale with the PNG output. Finally, in region D , beyond $620 \mu\text{s}$ there is constant ($\sim 150 \text{ counts/s}$) background composed mostly of γ s ($\geq 96\%$) due to fixed contamination, etc, unrelated to the PNG output.

Two runs were made, one with cavitation (i.e., the acoustic drive applied to the acetone chamber), and one without. In the 65-minute run with cavitation, 51 coincidences between pulses from the SL detector and the n/γ detector were observed; in the 58-minute run without cavitation, four coincidences were observed. These numbers are consistent with the expected random rates. Figure 2 shows the time distribution of singles and coincidences relative to the start of the PNG trigger pulse for the two runs. The coincidence event timing is defined by the neutron signal. Note that even with no cavitation there are light signals seen during the PNG pulse (region A). These are therefore not true SL signals.

The SL events during cavitation occur in four distinct regions shown in Figs. 2(a) and 2(b). The observed singles count rates in the n/γ detector within these four regions are quite different and must be known to calculate the expected random coincidence rates within the $20 \mu\text{s}$ coincidence window. Table I shows the results of such calculations. The number and time distributions of observed coincidences agree with the calculated random coincidence rates.

Figure 4 shows the distribution of time intervals between SL and n/γ pulses that were in coincidence (within $10 \mu\text{s}$

TABLE I. Estimated Random Coincidences

Reg.	$n\gamma$ rate cts/s	Probability of random coinc. in $20 \mu\text{s}$	Total SL events	Predicted SL- $n\gamma$ random coinc.	Observed SL/ $n\gamma$ coinc.
A	89	0.001 78	409	0.72 ± 0.4	1
B	3915	0.078 30	424	33.20 ± 1.62	29
C	953	0.019 06	47	0.89 ± 0.13	1
D	153	0.003 06	6983	21.37 ± 0.26	20
Total				56.20 ± 1.60	51 ± 7

of each other). As expected for random coincidences, there is no evidence for any clustering of events in time.

Note that the $n\gamma$ events in region A (Fig. 2(b)) were almost entirely eliminated by the $20 \mu\text{s}$ blocking pulse. In the absence of the blocking, essentially 100% of the SL signals in region A would fall within $\pm 10 \mu\text{s}$ of an $n\gamma$ count occurring during the PNG pulse and register as an $n\gamma$ -SL coincidence. These 400 coincidences would also exhibit a peaked time structure defined by the shape of the PNG pulse, unlike the others, shown in Fig. 4 that are scattered randomly throughout the $20 \mu\text{s}$ coincidence window. The coincidence technique used in Ref. [6] would be dominated by such events, which must be measured and then subtracted before any real coincidence events can be inferred from the data.

Taleyarkhan *et al.* [6] report seeing more neutrons in their singles data during runs with cavitation as compared to those without. We have examined our data to look for this effect and note a difference of 740 ± 290 counts in the 20 to $220 \mu\text{s}$ period following the PNG pulse in our $n\gamma$ singles during the run with cavitation as compared to the

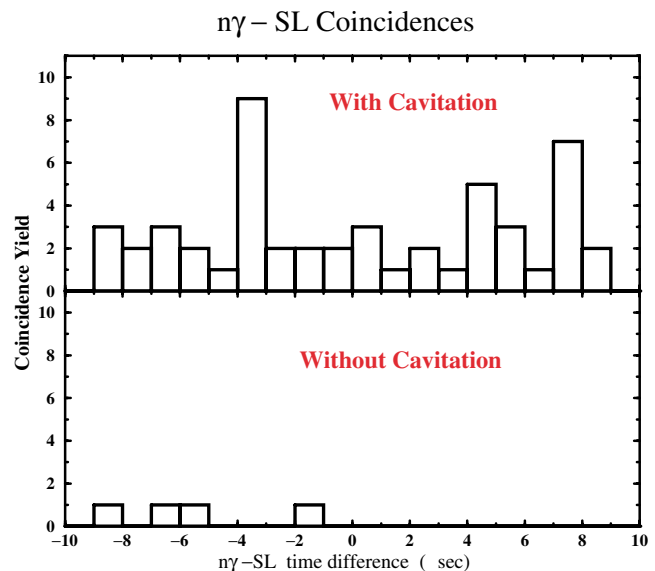


FIG. 4 (color online). Distribution of time intervals between SL and n/γ pulses. The original data had much higher dispersion, 5 ns/channel, and showed no structure on that time scale.

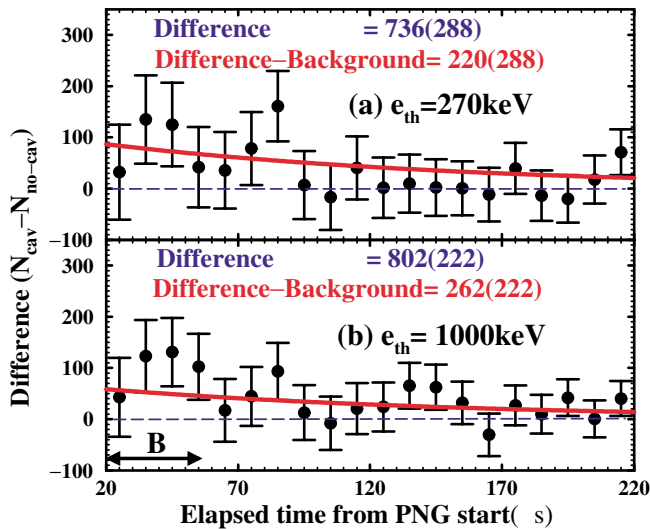


FIG. 5 (color online). Difference in n/γ counts (summed in $10 \mu\text{s}$ bins) with and without cavitation. The curve, represented by the solid line, corresponds to 2.5% of the room return background. The data shown have equivalent neutron thresholds of 1.2 MeV (a) and 2.8 MeV (b). Two numerical values for the difference are displayed in each figure. On top is the difference assuming a constant unchanging background. The values listed below as “Difference-Background” show the difference relative to an assumed change of 2.5% in room return background. The data fit this curve reasonably well. Also indicated is the time region (B in Fig. 2(b)) of initial bubble collapse.

run without cavitation. This difference amounts to about 2.5% of the room return background component and is significant if one considers only counting statistics as a source of uncertainty. A more detailed view of this difference is shown in Fig. 5(a). The statistical uncertainties are also indicated. The solid line shows the expected difference if the room return background during cavitation were to be increased by 2.5%, as might be expected from a variation in the PNG intensity (which was not monitored contemporaneously), or possibly a change in neutron scattering geometry due to people in the area being at different positions for the two runs.

The data shown in Fig. 5(a) were for our lowest threshold (~ 1.2 MeV neutrons). In Fig. 5(b) we show the difference spectrum for the data rescanned with a higher threshold of 2.8 MeV neutrons applied to the $n\gamma$ pulse-height spectrum. The data show essentially the same features, implying that the excess counts are due to events that deposit considerably more energy than 2.5-MeV neutrons, and consistent with the background due to $n-p$ capture gammas.

From these data, we can put an upper limit on the number of 2.5-MeV neutron events correlated with the SL light that might be in our data. This limit is approximately 100 counts (see Fig. 5(a)) accumulated in about 1 h. Using our estimate of detector efficiency for 2.5-MeV neutrons (0.3), applying the solid angle factor appropriate

for the detector geometry (2.5×10^{-2}), and allowing for transmission through the acetone, refrigeration material, and enclosure walls (0.35), we estimate the efficiency for detection of 2.5-MeV neutrons emitted from the acetone to be 2.5×10^{-3} , which would correspond to a source rate ≤ 100 neutrons/s, about 4 orders of magnitude below the rate implied by the tritium production reported in Ref. [6].

In the period during the PNG pulse the time resolution of the $n-\gamma$ electronics deteriorated due to the high instantaneous count rate. This resulted in poor $n-\gamma$ pulse shape discrimination in the period immediately after the PNG pulse. This was not the case in the time region between 700 and $1700 \mu\text{s}$ (see Fig. 2(a)) where about 80% of the SL light pulses appear. They appear in our data as sharp peaks $5 \mu\text{s}$ wide (FWHM) separated by the acoustic wave period of $52 \mu\text{s}$, and would be an interesting area for future study. In this time range no excess neutron yield was detected for runs with cavitation and we did not observe any correlation between the neutron yield and the emitted SL light pulse.

We conclude that there is no evidence of any real coincidences in this experiment. Furthermore, there is a substantial random coincidence rate, which must be properly allowed for in any attempt to identify real coincidences. The singles rates seen by both detectors must be measured contemporaneously in order to properly evaluate the random coincidence rate.

The observed excess of nuclear radiation seen during the run with cavitation appears to be due to a $\sim 2.5\%$ increase in room return background. It prevails at pulse heights corresponding to neutron energies in excess of 2.5 MeV, and is consistent with the characteristics of $n-p$ capture gammas.

We also note the intriguing time dependence seen in the SL detector.

We thank R. Varner for help in setting up the data acquisition system, and J.D. Fox and L. Berry for help with the manuscript. This research was sponsored by the Office of Science, U.S. Department of Energy under Contract No. DE-AC05-00OR22725 managed by UT-Battelle, LLC.

- [1] S. Putterman, *Sci. Amer.* **272**, 46–51 (1995).
- [2] B.P. Barber and S.J. Putterman, *Nature (London)* **352**, 318–323 (1991).
- [3] L. Crum and T. Matula, *Science* **276**, 1348 (1997).
- [4] Vasquez *et al.*, *Opt. Lett.* **26**, 575 (2001).
- [5] B. Barber *et al.*, *Phys. Rev. Lett.* **72**, 1380 (1994).
- [6] R.P. Taleyarkhan, C.D. West, J.S. Cho, R.T. Lahey, R.J. Nigamutin, and R.C. Block, *Science* **295**, 1868 (2002).
- [7] J.W. McConnell, R.L. Varner, W.T. Milner, and C.N. Thomas, *Physics Division Progress Report for period ending Sep. 30, 1992*, Report No. ORNL-6746, pp. 15–19.
- [8] J. Harvey and N. Hill, *Nucl. Instrum. Methods Phys. Res.* **162**, 507 (1979).
- [9] See <http://www.bicron.com/bc501A.htm>